

Temperature Dependent Photoluminescence Study on ZnO Nanostructures

Krisana Chongsri^{1,*}, Amara Kiewrugs¹, Kanuengnit Chuienkha² Theerayut Junkhiew³, Taweesub Juepanit⁴ and Apichart Sungthong¹

¹Department of Applied Physics, Faculty of Science and Technology, Rajabhat Rajanagarindra University, Chachoengsao 24000, Thailand

²Occupational Health and Safety Program, Faculty of Science and Technology, Rajabhat Rajanagarindra University, Chachoengsao 24000, Thailand

³Information Technology Program, Faculty of Science and Technology, Rajabhat Rajanagarindra University, Chachoengsao 24000, Thailand

⁴Chemistry Program, Faculty of Science and Technology, Rajabhat Rajanagarindra University, Chachoengsao 24000, Thailand

Abstract

In this paper, we studied the temperature dependent optical properties of ZnO nanostructures grown by hydrothermal process. The temperature dependent optical properties are significant feature for near band edge and deep-level emission mechanisms of ZnO nanostructures. Good ZnO nanostructures can result to donor bound exciton (D^0X) peak that can be measured by low temperature photoluminescence spectrum. Moreover, the morphologies and structural properties of ZnO nanostructures were investigated by X-ray diffraction (XRD) and Field emission scanning electron microscope (FE-SEM), respectively.

Keywords: Photoluminescence, ZnO nanostructures, X-ray diffraction

1. Introduction

Zinc Oxide (ZnO) is a wide band gap material (E_g) \sim 3.2-3.4 eV at 300 K with large exciton binding energy (\sim 60 meV) and typical n-type semiconductor [1]. ZnO has many advantages over other materials such as low cost, high stability and efficient excitonic emission. Nanostructures can be typically obtained by various growth techniques such as sol-gel process [2], hydrothermal process [3], radio frequency magnetron sputtering [4] and co-precipitation process [5]. Hydrothermal technique is one of dominating and effective processes due to their low temperature processing and ease of equipment set-up [6]. Nanoelectronics-based devices have been extensively studied in one-dimensional (1D) nanostructures because desirous shape and size of nanomaterials with exceptional properties can lead to their many appropriate applications. Therefore, 1D Zinc oxide (ZnO nanostructures) can be used for many applications such as UV detector devices [7], ultraviolet light-emitting devices [8] and transparent conductive oxide [9]. In this work, the formation of ZnO nanostructures grown by hydrothermal process is verified by photoluminescence spectroscopy. Photoluminescence measurement was conducted at various temperatures from 25K to 285K in order to investigate the important temperature-dependent parameters of this structure.

2. Experimental details

ZnO nanostructures grown on ZnO seeding layers were synthesized by hydrothermal process. The ZnO seeding layer was deposited by dip-coating technique. The precursor

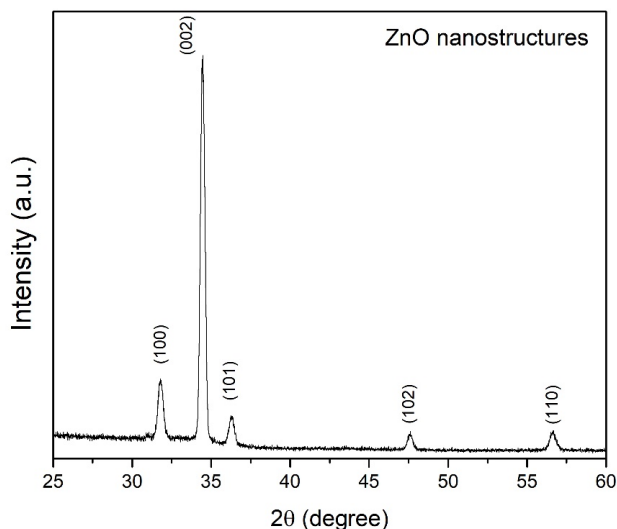


Fig. 1. X-ray diffraction pattern of ZnO nanostructures grown on ZnO seeding layer.

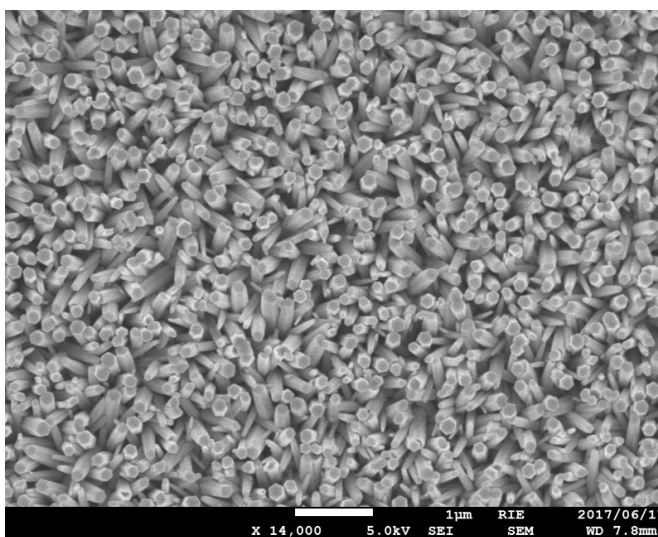


Fig. 2. FE-SEM micrograph of ZnO nanorods grown on ZnO seeding layer.

solution was then dip-coated onto cleaned glass substrates and annealed for 15 min at 100°C on a hot-plate and repeated for 10 times. Finally, the coated films were annealed in a furnace at 500°C for 2 h to form ZnO seeding layer. The ZnO nanostructures were synthesized by hydrothermal process. The solution for the synthesis of ZnO nanostructures was prepared by 100 mL of 0.05 M zinc nitrate hexahydrate ($Zn(NO_3)_2 \cdot 6H_2O$) and hexamethylenetetramine (HMTA) into 50 mL deionized water. The ZnO-seeded substrates dipped into the prepared solution and loaded in a Teflon autoclave for the hydrothermal reaction operating at 90°C for 2 h. Finally, the obtained white solid product was separated from the solution by sonication, washed with distilled water, and dried at 100°C for 24 h. The crystal structures and

morphologies of all samples were observed by XRD (Bruker D8 discover diffractometer) and FE-SEM (Hitachi S-4700), respectively. The optical properties were investigated by Photoluminescence spectroscopy (set up at Shizuoka university).

3. Results and discussion

Figure 1 shows the X-ray diffraction patterns of ZnO nanostructures growth on ZnO seed layer. The clearly seen diffraction peaks positioned at $2\theta = 31.77^\circ$, 34.42° , 36.25° , 47.54° and 56.60° are assigned to (100), (002), (101), (102) and (110) orientation planes of ZnO with hexagonal wurtzite structure, respectively (JCPDS card No. 36-1451). Fig. 2 illustrates the FE-SEM images of ZnO nanorods showing that hexagonal nanorods are well-grown on seed layers. The sample has hexagonal shape with the rod's diameter size in the range of 50-150 nm.

Figure 3 shows photoluminescence spectra of ZnO nanorods grown on ZnO seed layer measured as a function of temperature ranging from 25 K to 285 K. It can be observed that all PL spectra obtained have similar features including three sharp UV emission bands (360-400 nm) and a broad yellow-orange emission band (500-700 nm; at 285 K). The temperature dependent energy gap of semiconductor material is typically expressed in term of empirical relations proposed by many analytical models. It is clearly seen in fig. 3 that there is significant red-shift of major peak of UV-emission with increasing temperature. The relationship of major PL peak position with respect to temperature can be explained by the Vashni empirical model explained by the following equation.

$$E_g(T) = E_g(0K) - \alpha \frac{T^2}{\beta + T} \quad (1)$$

When $E_g(T)$ is the energy gap at temperature T , α and β are parameters to fit the experimental data (referred to as Vashni thermal coefficients) [10].

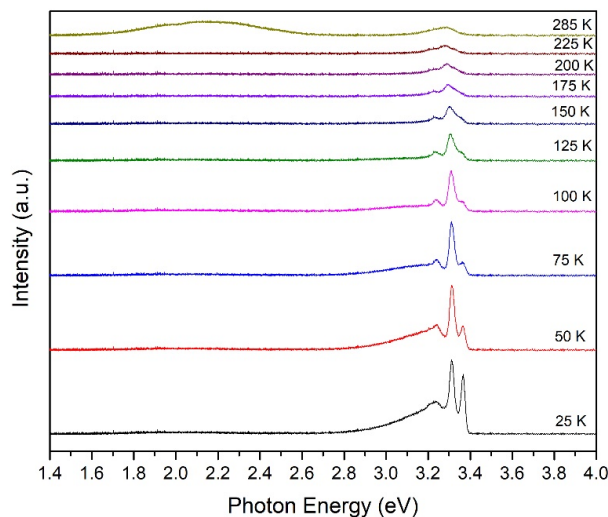


Fig. 3. PL spectra of the ZnO nanorods at 25 K to 285 K.

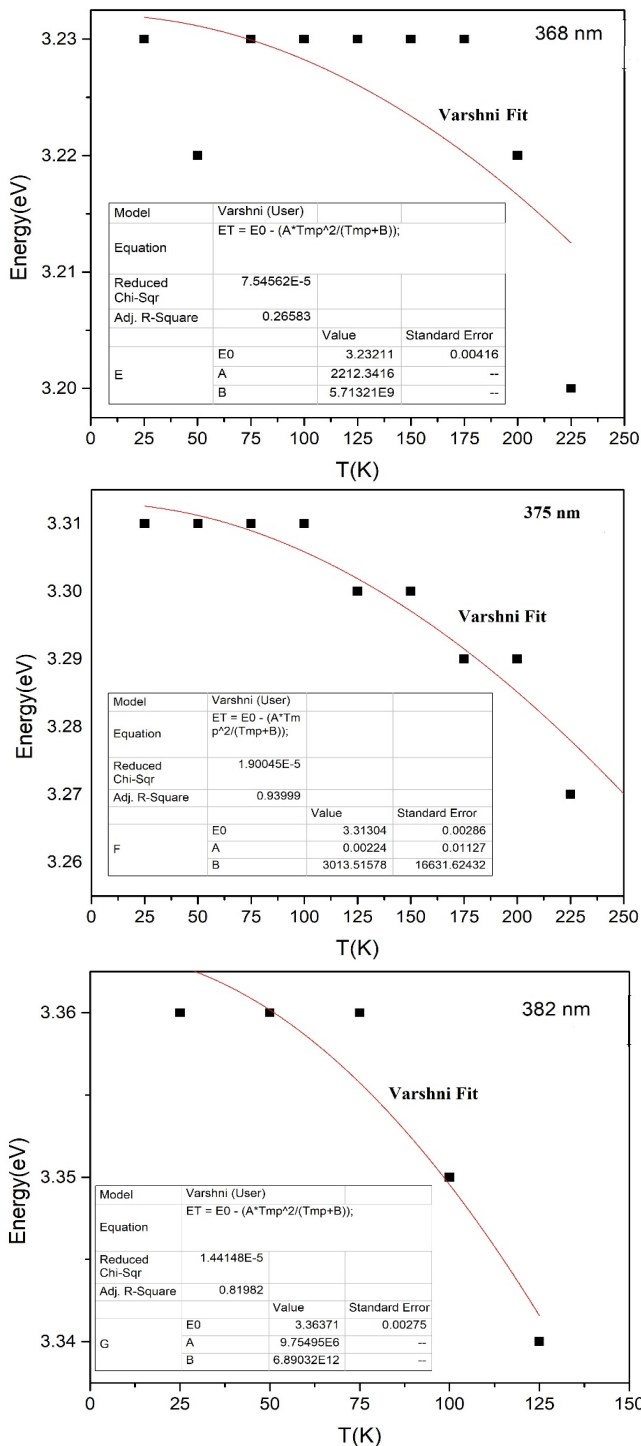


Fig. 4. Temperature dependent PL spectra of ZnO nanorods with curve fitting of three sharp UV emission bands ~368 nm, ~375 nm and ~382 nm.

Figure 4 shows temperature dependent PL spectra of ZnO nanorods with curve fitting of three sharp UV emission bands ~368 nm, ~375 nm and ~382 nm based on Vashni model. It is found that the best fitting process is exhibited in figure 4 (~375). It can be seen the fitting curve is in good agreement with the exciton of bound shallow neutral donor (D^0X) at ~375 nm. Furthermore, the broadening of this near band edge emission with increasing operating temperature is also noticed that may due to the natural temperature-induced broadening mechanism in semiconductor. Moreover, the first peak with shortest wavelength of ~368 nm is correlated to free exciton emission (FX). Third peak situated at ~382 nm with broad shoulder can be attributed to the donor to bound exciton emission. At 285 K shows yellow-orange emission band (500-700 nm) of ZnO nanorods. The intensity of yellow-orange emission component increases when the high temperature, indicating that the yellow-orange emission is closely associated with the electron-phonon interaction and thermal expansion of the lattice, which inhibits the UV emission [11-12].

4. Conclusion

The ZnO nanostructures was successfully grown by hydrothermal process. The results of Temperature Dependent Photoluminescence (25 K to 285 K) of the ZnO nanostructures are composed of UV emission bands and yellow-orange emission band. The three sharp UV emission bands spectra qualitatively suggest the existence of the ZnO structures. All results indicated that the band gap energy of ZnO nanorods are assumed to be dependent to temperature and good morphologies which produces a high uniform and highest density growth of ZnO nanostructures confirm by XRD and FE-SEM, respectively.

Acknowledgement

This work has been supported by the Nano Materials Research Laboratory (NMRL). The authors would like to thank College of Nanotechnology, King Mongkut's Institute of Technology Ladkrabang and Department of Applied Physics, Faculty of Science and Technology, Rajabhat Rajanagarindra University Chachoengsao for financial supports.

References

- [1] Thirunavukkarasu K, Jothiramalingam R. Synthesis and structural characterization of Ga-ZnO nanodisk/nanorods formation by polymer assisted hydrothermal process. *Powder Technol.* 2013;239:308-313.
- [2] Valencia S, Marín JM, Restrepo G. Study of the bandgap of synthesized titanium dioxide nanoparticules using the sol-gel s. method and a hydrothermal treatment. *The Open Mat. Sci. J.* 2009;4:9-14.
- [3] Hua-Rui X, Huaiying Z, Guisheng Z, Jinzhong C, Chuntu L. Synthesis of tin-doped indium oxide nanoparticles by an ion-exchange and hydrothermal process. *Mater. Lett.* 2006;60(7):983-985.
- [4] Yang CH, Lee SC, Lin TC, Zhuang WY. Effect of tin doping on the properties of indium-tin-oxide films deposited by radio frequency magnetron sputtering. *Mat. Sci. Eng. B.* 2007;138(3):271-276.
- [5] Seetha M, Bharathi S, Dhayal RA. Optical investigations on indium oxide nano-particles prepared through precipitation method. *Mater. Charact.* 2009;60(12):1578-1582.
- [6] Xian F, Bai W, Xu L, Wang X, Li X. Controllable growth of ZnO nanorods by seed layers annealing using hydrothermal method. *Mat. Lett.* 2013;108:46-49.

-
- [7] Vaishnav VS, Patelv SG, Panchal JN. Development of ITO thin film sensor for detection of benzene. *Sens. Actuators B Chem.* 2015;206:381-388.
- [8] Jongwoon P, Hyokyun H. Sputter-patterned ITO-based organic light-emitting diodes with leakage current cut-off layers. *Org. Electron.* 2011;12(11):1872-1878.
- [9] Jeong JA, Jeon YJ, Kim SS, Kim BK, Chung KB, Kim HK. Simple brush-painting of Ti-doped In₂O₃ transparent conducting electrodes from nano-particle solution for organic solar cells. *Sol. Energ. Mat. Sol. C.* 2014;122:241–250.
- [10] Liu X, Huang DL, Wu LL, Zhang XT, Zhang WG. Novel photoluminescence properties of InAlO₃(ZnO)_m superlattice nanowires. *Chin. Phys. B.* 2011;20(7):078101.
- [11] Liping Z, Jiasheng L, Zhizhen Y, Haiping H, Xiaojun C, Binghui Z. Photoluminescence of Ga-doped ZnO nanorods prepared by chemical vapor deposition. *Opt. Mater.* 2008;31(2):237–240.
- [12] Bandopadhyay K, Mitra J. Zn interstitials and O vacancies responsible for type ZnO: what do the emission spectra reveal. *RSC Adv.* 2015;5(30):23540.